Electron temperature analysis of two-gas-species inductively coupled plasma

K. H. Bai, H. Y. Chang, and H. S. Uhm

Citation: Appl. Phys. Lett. **79**, 1596 (2001); doi: 10.1063/1.1404135
View online: http://dx.doi.org/10.1063/1.1404135
View Table of Contents: http://apl.aip.org/resource/1/APPLAB/v79/i11
Published by the American Institute of Physics.

Electron temperature analysis of two-gas-species inductively coupled plasma

K. H. Bai[a] and H. Y. Chang
Department of Physics, Korea Advanced Institute of Science and Technology, Taejon 305-701, South Korea

H. S. Uhm
Department of Molecular Science and Technology, Ajou University, Suwon 442-749, South Korea

(Received 3 January 2001; accepted for publication 18 July 2001)

The electron energy distribution functions and electron temperatures are measured in Ar/He and Ar/Xe inductively coupled plasma with various mixing ratios. The electron temperature does not change linearly with the mixing ratios; instead it increases abruptly near $P_{\mathrm{He}}/P_{\mathrm{Ar+He}}=1$ and decreases rapidly near $P_{\mathrm{Xe}}/P_{\mathrm{Ar+Xe}}=0$. A simple model using a two-ion-species fluid model is suggested to explain the electron temperature variations, and it agrees well with the experimental results. © *2001 American Institute of Physics.* [DOI: 10.1063/1.1404135]

Usually processes are done using two or more gas species simultaneously. For example, in the silicon dioxide etching process, Ar, Xe, or H_2 are added to various fluorocarbon gases to increase the etching selectivity to Si underlayer,[1] and a Ne and Xe mixture is used in plasma display panel (PDP) cells for easy breakdown and high lighting intensity. Another example of gas mixture is the addition of rare gases as a trace rare gas (TRG) to determine plasma properties such as the electron energy distribution function (EEDF) of a high energy tail.[2] Studies on gas mixture effects have been done by a number of researchers. Ishikawa *et al.* have reported the ionic species intensity variation in CF_4/Ar plasmas as a function of the Ar mixing ratio.[3] Kobayashi *et al.* have reported the variation of discharge-sustaining voltage (DSV), the phase angle ϕ of the discharge current to the applied voltage and the electron temperature (T_e) with various gas mixing ratios in CF_4/N_2 plasma.[4]

Electron temperature is one of the most interesting plasma parameters because it is believed to be related to undesirable effects like notching, charge buildup, and radical composition.[5–7]

It is well known that the electron temperature increases and the electron density decreases when a gas of higher ionization threshold energy is added, and vice versa. The electron temperature and other plasma parameters do not change linearly with the mixing ratio, especially when the mixed gas has a very different threshold ionization energy or mass. Consequently it is difficult to predict the values of the electron temperature and other plasma parameters versus the gas mixing ratio. However, obtaining plasma parameters in a single gas system is not so difficult. They can be obtained from a simple experiment or from the wealth of published data.

This letter assumes that we know the electron temperature when plasma is discharged by a single gas, i.e., the mixing ratio is 0% or 100%, and we try to analyze the electron temperature when the mixing ratio is between 0% and 100%. We propose a two-ion-species fluid model in comparison with the experimental results. The EEDFs are measured to calculate effective electron temperatures using a rf-compensated Langmuir probe in Ar/He 20 mTorr and Ar/Xe 10 mTorr ICP at various mixing ratios.

The ICP reactor used in this study has been described in a previous paper.[8] The discharge chamber consists of two regions: one has a Pyrex cylinder 15 cm in diameter, 12 cm long, and a grounded stainless steel cylinder 22 cm in diameter, 10 cm long; the other region is for another purpose and has no effects on the first region.[8] For precise pressure measurement, a capacitive manometer (MKS, 127AA-00001B) is used. 600 W, 13.56 MHz rf power is coupled to a single-turn copper coil. A rf-compensated Langmuir probe, set at the center of the reactive chamber, measures the EEDFs $[F(\epsilon)]$, effective electron temperatures ($T_{\mathrm{eff}}=2/3\langle\epsilon\rangle$), electron densities $[n_e=\int F(\epsilon)d\epsilon]$, and plasma potentials. To reduce the rf distortion of the probe characteristics, a probe system consisting of a small measurement probe and a floating-loop reference probe with a resonant filtering technique is used.[9] The ac measurement technique with a lock-in amplifier is used, because it has the advantage of low output noise.[9–11] The energy difference (Δ) between the zero crossing point and the peak point of the EEDFs indicates signal quality and reliability.[9,12] In this experiment, the energy difference (Δ) is less than 1 eV even in the worst case, which demonstrates the accuracy of the measurement.

Figure 1 shows the experimental results of the electron energy probability functions (EEPFs) change with various He mixing ratios in Ar/Hr plasma. The EEPFs show two temperature structures due to inelastic collisions and fast electron escape to the chamber wall. This two temperature structure is shown in other experiments.[8,12,13]

Though this non-Maxwellian EEPF structure may cause problems, EEPF is assumed to be Maxwellian generally in fluid modeling for simple calculation.[14–18] In this letter we also assume Maxwellian EEPF with effective electron temperature T_e. Note that the effective electron temperature increases with the He mixing ratio, but it does not increase linearly with the He mixing ratio; instead, it varies abruptly near $\kappa=P_{\mathrm{He}}/P_{\mathrm{He+Ar}}=1$. We use a fluid model to analyze this electron temperature variation. Electron temperatures are

[a]Electronic mail: bazarofe@kaist.ac.kr

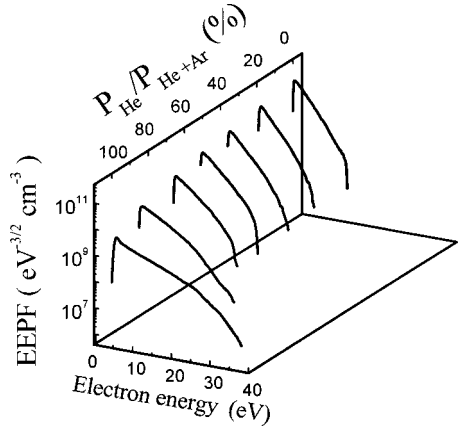

FIG. 1. EEPFs variation as a function of the P_{He} ratio in Ar/He plasma.

determined by equating the total particle loss to the total volume ionization as follows:

$$\frac{K_{iz}(T_e)}{u_B(T_e)}=\frac{1}{n_g d_{\mathrm{eff}}},\quad d_{\mathrm{eff}}=\frac{1}{2}\frac{Rl}{Rh_l+lh_R},\tag{1}$$

where K_{iz} is an ionization rate constant, u_B is the Bohm velocity of ion, n_g is the neutral density, R,l are the chamber radius and length, respectively, and h_l, h_R are the ratios of electron density at edge to electron density at center, and d_{eff} is an effective plasma size which is a function of the ion-atom scattering cross section σ_i,[19] for argon $\sigma_i=10^{-14}\,\mathrm{cm}^2$ and $\sigma_i=5\times10^{-15}\,\mathrm{cm}^2$, $\sigma_i=2\times10^{-14}\,\mathrm{cm}^2$ for He and Xe, respectively.[20] In our experiment the electron temperature variation due to the variation of d_{eff} is at most a few percent. Thus in the letter, we assume d_{eff} is constant.

Equation (1) describes the relations between electron temperature and ionization rate constant and Bohm velocity when there are only one species of ions and neutral gas in plasma. To determine the electron temperature using Eq. (1) in a two-or-more-ion-species system, the total ionization rate constant and the Bohm velocity should be defined.

When the discharge gas consists of two gas species α, β, and their partial pressure ratio is $1-\kappa:\kappa$, we can define the total ionization rate constant (K_t) as

$$K_t=(1-\kappa)K_\alpha+\kappa K_\beta,\tag{2}$$

where subscript α denotes the value of α, β denotes the value of β and subscript t denotes the sum of them; for example, K_α is the ionization rate constant of α. When EEDF is an isotropic Maxwellian distribution and T_e is much smaller than the ionization threshold energy (ϵ_{iz}) and excitation threshold energy (ϵ_{ex}) of the neutral, it is possible to approximate K_{iz} as

$$K_{iz}(T_e)=\sigma_0\overline{v_e}\left(1+\frac{2T_e}{\epsilon_{iz}}\right)e^{-\epsilon_{iz}/T_e},\tag{3}$$

where $\overline{v_e}=(8eT_e/\pi m)^{1/2}$, $\sigma_0=\pi(e/4\pi\epsilon_0\epsilon_{iz})^2$, and m is electron mass.[19] Inserting Eq. (3) into Eq. (2), we obtain

$$K_t=(1-\kappa)\sigma_\alpha\overline{v_e}\left(1+\frac{2T_e}{\epsilon_{iz,\alpha}}\right)e^{-\epsilon_{iz,\alpha}/T_e}+\kappa\sigma_\beta\overline{v_e}\times\left(1+\frac{2T_e}{\epsilon_{iz,\beta}}\right)e^{-\epsilon_{iz,\beta}/T_e},\tag{4}$$

where σ_α and σ_β are σ values of α and β.

If α^+ and β^+ are the main ion species and the two ion species have their own Bohm velocities $u_{B,\alpha}=\sqrt{T_e/M_\alpha}$, $u_{B,\beta}=\sqrt{T_e/M_\beta}$, then we can define average Bohm velocity $u_{B,\mathrm{avg}}$ as

$$\Gamma_t=n_\alpha u_{B,\alpha}+n_\beta u_{B,\beta}=n_t u_{B,\mathrm{avg}}\tag{5}$$

where Γ_t is the total ion loss rate to walls. n_α, n_β, n_t are the ion densities of α^+, β^+, and the sum of them at the sheath edge, respectively.

Each ion density is proportional to its ionization rate constant and its mixing ratio, then Eq. (5) can be reduced as

$$u_{B,\mathrm{avg}}=\frac{(1-\kappa)K_\alpha}{(1-\kappa)K_\alpha+\kappa K_\beta}u_{B,\alpha}+\frac{\kappa K_\beta}{(1-\kappa)K_\alpha+\kappa K_\beta}u_{B,\beta}.\tag{6}$$

Inserting Eqs. (4) and (6) into Eq. (1), we obtain

$$\frac{[(1-\kappa)\sigma_\alpha(1+2T_e/\epsilon_\alpha)e^{-\epsilon_\alpha/T_e}+\kappa\sigma_\beta(1+2T_e/\epsilon_\beta)e^{-\epsilon_\beta/T_e}]^2}{(1-\kappa)(1+2T_e/\epsilon_\alpha)e^{-\epsilon_\alpha/T_e}\sqrt{1/M_\alpha}+\kappa\sigma_\beta/\sigma_\alpha(1+2T_e/\epsilon_\beta)e^{-\epsilon_\beta/T_e}\sqrt{1/M_\beta}}=\frac{1}{n_g d_{\mathrm{eff}}}\left(\frac{8}{\pi m}\right)^{-1/2}.\tag{7}$$

The rhs of Eq. (7) is constant, and after inserting $\kappa=0$, Eq. (7) can be reduced as

$$\frac{[(1-\kappa)(1+2T_e/\epsilon_\alpha)e^{-\epsilon_\alpha/T_e}+\kappa\sigma_\beta/\sigma_\alpha(1+2T_e/\epsilon_\beta)e^{-\epsilon_\beta/T_e}]^2}{(1-\kappa)(1+2T_e/\epsilon_\alpha)e^{-\epsilon_\alpha/T_e}+\kappa\sigma_\beta/\sigma_\alpha(1+2T_e/\epsilon_\beta)e^{-\epsilon_\beta/T_e}\sqrt{M_\alpha/M_\beta}}=\left(1+\frac{2T_{0,\alpha}}{\epsilon_\alpha}\right)e^{-\epsilon_\alpha/T_{0,\alpha}},\tag{8}$$

where $T_{0,\alpha}$ is the electron temperature when $\kappa=0$ or $P_{\mathrm{He}}/P_{\mathrm{Ar+He}}=0\%$. Inserting $\kappa=0$ in Eq. (8), T_e becomes $T_{0,\alpha}$. $\sigma_\beta/\sigma_\alpha=(\epsilon_\alpha/\epsilon_\beta)^2$; but we can obtain the value also using Eq. (3) and $K_\alpha/u_\alpha=K_\beta/u_\beta$ as

$$\frac{\sigma_\beta}{\sigma_\alpha}=\sqrt{\frac{M_\alpha}{M_\beta}}\left(\frac{1+2T_{0,\alpha}/\epsilon_\alpha}{1+2T_{0,\beta}/\epsilon_\beta}\right)e^{-(-\epsilon_\alpha/T_{0,\alpha}-\epsilon_\beta/T_{0,\beta})}\tag{9}$$

where $T_{0,\beta}$ is the electron temperature when $\kappa=1$ or $P_{\mathrm{He}}/P_{\mathrm{Ar+He}}=100\%$. Using Eq. (9), T_e becomes $T_{0,\beta}$ when $\kappa=1$. Finally, it is possible to obtain electron temperature as a function of κ by using Eqs. (8) and (9). Figure 2 shows the electron temperature variation as a function of the He ratio in the Ar/He mixture plasma with a total pressure of 20 mTorr and 600 W, where the solid line represents the calculated

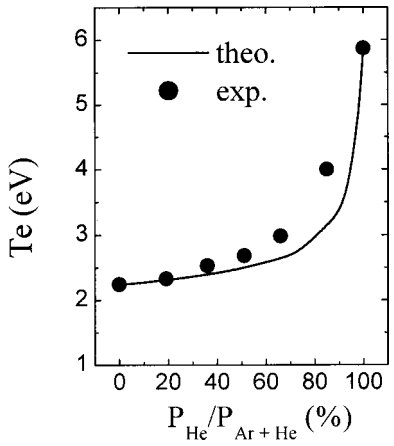

FIG. 2. Theoretical (solid line) and experimental (broken line) result of electron temperature as a function of the P_{He} ratio in Ar/He plasma.

values using Eq. (8), and the broken lines are experimental values. Though there is a small disagreement near $\kappa=1$, the calculated values agree well with the experimental values. Figure 3 shows the results of the Ar/Xe mixture. The electron temperature decreases with κ, and it decreases rapidly near $\kappa=0$.

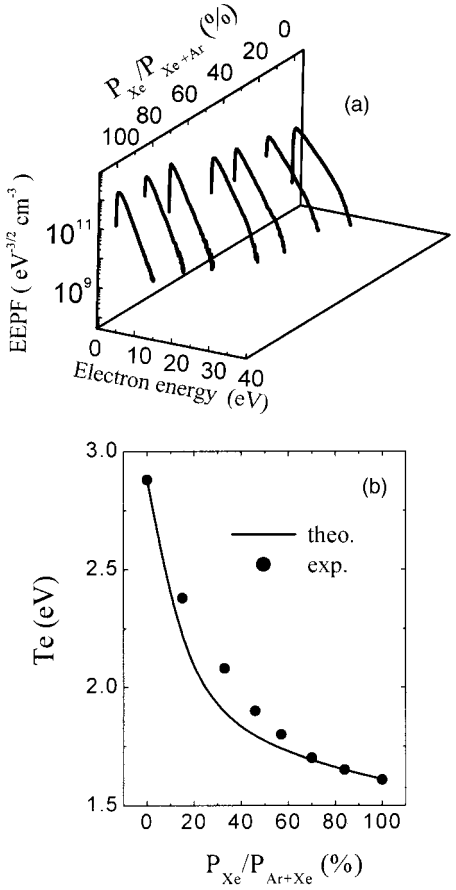

FIG. 3. Results in Ar/Xe plasma. (a) The EEPFs evolutions as a function of the P_{Xe} ratio; (b) theoretical (solid line) and experimental (broken line) results of electron temperature as a function of the P_{Xe} ratio.

The EEDFs and electron temperatures as a function of the mixing ratios in Ar/He at 20 mTorr and Ar/Xe at 10 mTorr are measured using a compensated Langmuir probe. The electron temperatures do not change linearly with the He and Xe mixing ratios, but electron temperature increases abruptly at $\kappa=1$ in Ar/He plasma and it decreases rapidly near $\kappa=0$ in Ar/Xe plasma. It may be possible to say that electron temperature changes more effectively when the mixed gas has a large ionization cross section and large mass due to its high ionization rate and slow Bohm velocity. Using a two-ion-species fluid model, electron temperature variation as a function of the mixing ratio can be calculated, which agrees well with the experimental results. In this model we assume EEDFs are Maxwellian and d_{eff} is constant. We think such assumptions cause the difference between calculated and measured electron temperature because measured EEDFs show they are non-Maxwellian, and d_{eff} varies with mixing ratio. We also neglect reactions between different ion species which may be another reason for the discrepancy. This model may be used in a system with other gas mixtures. Electron density and plasma potential are also important plasma parameters for plasma processes. Though not shown in this letter, the measured plasma potentials show similar trends with electron temperatures, but electron densities show different trends and consequently more study is needed to analyze these trends.

[1] H. Sugai and K. Nakamura, J. Vac. Sci. Technol. A **13**, 887 (1995).
[2] T. Nakano and S. Samukawa, J. Vac. Sci. Technol. A **17**, 686 (1999).
[3] I. Ishikawa, S. Sasaki, K. Nagaseki, Y. Saito, and S. Suganomata, Jpn. J. Appl. Phys., Part 1 **17**, 4648 (1997).
[4] H. Kobayashi, I. Ishikawa, and S. Suganomata, Jpn. J. Appl. Phys., Part 1 **17**, 5979 (1994).
[5] N. Fujiwara, T. Maruyama, M. Yoneda, K. Tsukamoto, and T. Banjo, Jpn. J. Appl. Phys., Part 1 **17**, 2164 (1994).
[6] S. Samukawa, Y. Nakagawa, T. Tsukada, H. Ueyama, and K. Shinohara, Jpn. J. Appl. Phys., Part 1 **17**, 6805 (1995).
[7] S. Samukawa, Jpn. J. Appl. Phys., Part 1 **17**, 2133 (1994).
[8] J. I. Hong, S. H. Seo, S. S. Kim, N. S. Yoon, C. S. Chang, and H. Y. Chang, Phys. Plasmas **6**, 1017 (1999).
[9] V. A. Godyak, R. B. Piejak, and B. M. Alexandrovich, Plasma Sources Sci. Technol. **1**, 36 (1992).
[10] G. R. Branner, E. M. Friar, and G. Medicus, Rev. Sci. Instrum. **34**, 231 (1963).
[11] S. H. Seo, J. I. Hong, K. H. Bai, and H. Y. Chang, Phys. Plasmas **6**, 614 (1999).
[12] U. Kortshagen, I. Pukropski, and M. Zethoff, J. Appl. Phys. **76**, 2048 (1994).
[13] V. A. Godyak, R. B. Piejak, and B. M. Alexandrovich, Plasma Sources Sci. Technol. **4**, 332 (1995).
[14] J. T. Gudmundsson, T. Kimura, and M. A. Lieberman, Plasma Sources Sci. Technol. **8**, 22 (1999).
[15] T. Kimura and K. Ohe, Plasma Sources Sci. Technol. **8**, 553 (1999).
[16] S. Ashida, C. Lee, and M. A. Lieberman, J. Vac. Sci. Technol. A **13**, 2498 (1995).
[17] C. Lee, D. B. Graves, M. A. Lieberman, and D. W. Hess, J. Electrochem. Soc. **141**, 1546 (1994).
[18] C. Lee and M. A. Lieberman, J. Vac. Sci. Technol. A **13**, 368 (1995).
[19] M. A. Lieberman and A. J. Lichtenberg, *Principles of Plasma Discharges and Materials Processing* (Wiley, New York, 1994).
[20] P. Larsen and M. Elford, J. Phys. B **19**, 449 (1986).